

1 **The novel role of LOC344887 in the enhancement of hepatocellular carcinoma**
2 **progression via modulation of SHP1-regulated STAT3/HMGA2 signaling axis**

3

4 **Supplemental information**

5 **Supplementary materials and methods**

6 **Cell culture and reagents**

7 HepG2 (RRID:CVCL_0027), Huh7 (RRID: CVCL_0336), Hep3B
8 (RRID:CVCL_0326), J7 (RRID:CVCL_4Z69)(gift from Dr. C S Yang, National
9 Taiwan University, Taiwan)[1], Mahlavu (RRID:CVCL_0405), and SK-Hep1
10 (RRID:CVCL_0525) were cultured in Dulbecco's Modified Eagle's Medium (DMEM;
11 Gibco, New York, USA) supplemented with 10% fetal bovine serum (FBS; Gibco),
12 100 µg/mL streptomycin sulfate, and 100 IU/mL penicillin G. Cells were maintained
13 in an incubator at 37°C with a humidified atmosphere and 5% CO₂. Prior to
14 conducting in vitro assays, the cells were subjected to examination for mycoplasma
15 contamination using the TOOLS mycoplasma detection kit (BIOTOOLS, New Taipei
16 City, Taiwan, TTB-GBC8) to ensure their integrity.

17

18 **RNA extraction, reverse transcription polymerase chain reaction (RT-PCR) and**
19 **qRT-PCR**

20 To ascertain the transcript of the target gene, total RNA was isolated using TRIzol
21 reagent (Life Technologies Inc., Carlsbad, CA, USA). Subsequently, the RNA was
22 converted into cDNA through reverse transcriptase (Life Technologies). For the
23 RT-PCR analysis, a 20 μ L reaction was conducted with forward and reverse primers
24 and 1X DNA polymerase. The RT-PCR conditions included an initial denaturation at
25 95°C for 5 min, followed by 30 cycles of 95°C for 30 sec, 55°C for 30 sec, and 72°C
26 for 1 min. For the qRT-PCR analysis, a 15 μ L reaction was performed with forward
27 and reverse primers and 1X SYBR green master mix (Applied Biosystems, Carlsbad,
28 CA, USA). The standard qRT-PCR conditions were an initial denaturation at 95°C for
29 10 min, followed by 40 cycles of 95°C for 15 sec, and 60°C for 1 min. The primers
30 utilized in this study are listed in Supplementary Table 1.

31

32 **5' and 3' rapid amplification of cDNA ends (RACE) assays**

33 RACE experiments (Roche Diagnostics, Mannheim, Germany, Catalog No.
34 03343621001) followed the manufacturer's protocol. Briefly, the amplification of the
35 LOC344887 signal was performed through nested PCR using two sets of primers, as
36 listed in Supplementary Table 1. The PCR product was visualized by electrophoresis
37 and ligated into the pGEM-T easy vector for DNA sequencing. The sequences derived
38 from the sequencing results were aligned using the NCBI genome browser.

39 **Immunoblot analysis**

40 The immunoblot analysis protocol was executed following previously described
41 procedures [2]. The antibodies employed in this study are detailed in Supplementary
42 Table 2. Signal detection was accomplished using X-ray films for chemiluminescence
43 detection. Signal intensities were quantified using Image Gauge software. The
44 expression levels of the target genes were normalized to GAPDH.

45

46 ***In situ* hybridization**

47 The detection of the LOC344887 signal was performed using the RNAScope™
48 Detection Reagent Kit RED with a custom LOC344887 probe (Advanced Cell
49 Diagnostics, Hayward, CA, USA, #323970-USM). The LOC344887 signal was
50 visualized as a brown signal. The stained tissue array was scanned and observed using
51 NDP.view2 viewer. The intensity of LOC344887 in the tissue array was quantified
52 using Image J software.

53

54 **Immunohistochemical (IHC) staining**

55 The immunohistochemical staining protocol has been previously described [3].
56 Briefly, the primary antibodies used for IHC staining and their dilutions are listed in
57 Supplementary Table 2. Detection was performed using the EnVision kit (DAKO,

58 Carpinteria, CA, USA), with positive signals appearing as brown. The intensity of
59 p-STAT3 (Tyr705) and HMGA2 in tumor cells was categorized as absent (0), weak
60 (1+), moderate (2+), or strong (3+). Additionally, the percentage of positive cells was
61 classified as absent (0), focal ($\leq 10\%$), regional (11%-50%), or diffuse ($>50\%$). The
62 histoscore was calculated by multiplying the percentage of antibody-positive cells by
63 the intensity.

64

65 **Gene expression and pathway analysis**

66 Total RNA from LOC344887 knockdown J7 cell lines was isolated using TRIzol
67 reagent and analyzed for gene expression profiling with the Agilent SurePrint G3
68 Gene Expression Microarray (Agilent Technologies, Santa Clara, CA, USA). Signal
69 extraction was carried out using Feature Extraction software (version 10.7.3.1).
70 Differentially expressed genes regulated by LOC344887 were identified using their
71 official gene IDs and further subjected to KEGG pathway analysis using the
72 clusterProfiler (4.8.2) package.

73

74 **Cell proliferation**

75 LOC344887 stable cells (5×10^4) were seeded in 6 cm plates. After 24h, 48h, and 72h
76 of seeding, the cells stained with 0.4% trypan blue were determined using a cell

77 counter. The cell growth rate was normalized to day one and presented as a fold
78 change.

79

80 **Cell migration and invasion assay**

81 The Transwell assay (Becton-Dickinson, Franklin Lakes, NJ, USA, #3422) assessed
82 cell migratory and invasive capabilities. Cells (8×10^2 cells/ μ l) suspended in
83 serum-free medium were seeded in the upper chamber, which was either
84 non-matrigel-coated (for migration assay) or matrigel-coated (for invasion assay). In
85 contrast, the lower chamber contained DMEM with 20% FBS. After 18 hours of
86 incubation, migratory or invasive cells were fixed and stained using crystal violet.
87 Image J software quantified the cells traversing from the upper to the lower chamber.

88

89 **Establishment of target gene stable cell lines**

90 Full-length sequences of LOC344887 (v1 and v2), HMGA2, STAT3 (wild-type), and
91 SHP-1 were amplified by PCR and cloned into pcDNA3 expression plasmid
92 (Invitrogen, Carlsbad, CA, USA). The dominant-negative STAT3 (Y705F) pcDNA3
93 plasmid (Plasmid #74434) was purchased from Addgene. The pool stable
94 overexpression of those genes in hepatoma cell lines was incubated with DMEM with
95 10% FBS and G418 (800 μ g/ml). We also performed the transient transfection assays

96 (as described in the corresponding figure legend). The shRNAs targeted to the
97 LOC344887 (shLOC344887#1 and shLOC344887#2) were synthesized and cloned
98 into pLKO.1 vector based on the guidelines of the TRC shRNA design algorithm
99 (RNAi core). In addition, the HMGA2 and SHP-1 shRNAs were purchased from the
100 National RNA Interference Core Facility (Institute of Molecular Biology, Academia
101 Sinica, Taiwan). The lentivirus-targeted individual genes were prepared as described
102 previously [4]. The pool stable knockdown specific genes were incubated with
103 DMEM with 10% FBS and puromycin (0.5 $\mu\text{g}/\text{ml}$). The information on each shRNA
104 is listed in Supplementary Table 1.

105

106 **Animal models**

107 In tumor formation assay, Mahlavu-sh-luc#1 (1×10^6 cells, $n = 4$),
108 Mahlavu-shLOC344887#1 (1×10^6 cells, $n = 3$), J7-sh-luc#1 (2×10^6 cells, $n = 5$) and
109 J7-shLOC344887#1 (2×10^6 cells, $n = 5$) were injected into the nude mice,
110 respectively. Tumor volumes were analyzed by the formula $(W^2 \times L)/2$ (W, most minor
111 diameter, and L, longest diameter). In the metastatic assay, severe combined
112 immunodeficient (SCID) mice were used to investigate the metastatic effect of
113 LOC344887-depleted J7 cells. J7-sh-luc#1 and J7-shLOC344887#1 (2×10^6 , $n = 4$)
114 cells were intravenously injected into the SCID mice. Furthermore, SCID mice were

115 used to uncover the metastatic effect of the LOC344887/HMGA2 axis (rescue
116 experiment). J7-sh-luc#1/vc (n = 4), J7-shLOC344887#1/vc (n = 5),
117 J7-sh-luc#1/HMGA2 (n = 5), and J7-shLOC344887#1/HMGA2 (n = 5) cells (2×10^6)
118 were intravenously injected into the SCID mice. After H&E staining, the metastatic
119 tumor (relative fold) in the lungs was determined. All assays were performed
120 according to the United States National Institutes of Health guidelines and Chang
121 Gang Institutional Animal Care and Use Committee Guide for the Care and Use of
122 Laboratory Animals (IACUC: CGU109-135).

123

124 **Human JAK/STAT Pathway Phosphorylation Array**

125 The human JAK/STAT pathway phosphorylation array kit (Catalog
126 #AAH-JAKSTAT-1-4) was used following the manufacturer's protocol (RayBiotech
127 Life, Inc., Peachtree Corners, GA, USA). Briefly, 150 μ g of protein extracted from
128 control and LOC344887 knockdown cell lines was incubated with a blocking
129 membrane overnight at 4°C. The membranes were then washed with wash buffers I
130 and II. Afterward, the detection antibody cocktail was incubated with the membranes
131 overnight at 4°C. An HRP-conjugated antibody was applied for 2 hours at room
132 temperature. Chemiluminescence was used to detect the signals visualized on X-ray
133 film.

134 **Reporter assay**

135 The vector NTI software (Thermo Fisher Scientific) was employed to predict six
136 potential STAT3 binding sites (-1500/-1492, -912/-904, -866/-858, -503/-495,
137 -440/-432, and -414/-406) within the HMGA2 promoter region. Fragments of the
138 HMGA2 promoter (fragments I, II, III, IV, and VI) and a deletion of the putative
139 STAT3 binding site in the HMGA2 promoter (fragments V and VII) were amplified
140 using PCR and then cloned into the PGL3-TK vector. Hepatoma cells (3×10^4) were
141 seeded in a 24-well plate and co-transfected with pcDNA3, pcDNA3-LOC344887-v1,
142 pcDNA3-LOC344887-v2, HMGA2 reporter plasmids, and the β -galactosidase
143 plasmid (Clontec Laboratories Mountain View, CA, USA) using TurboFectTM
144 (Thermo Fisher Scientific). Luciferase activity was normalized to the control vector.
145 In addition, the STAT3 reporter activity was determined using STAT3 Reporter Assay
146 Kit (BPS Bioscience, San Diego, CA, USA, #79730).

147

148 **Chromatin immunoprecipitation (ChIP) assay**

149 This assay was performed on the HMGA2 promoter region following a previously
150 described protocol [2]. Briefly, hepatoma cells overexpressing vector control,
151 LOC344887-v1, and LOC344887-v2 were harvested and cross-linked with 1%
152 formaldehyde. The reaction was terminated by adding 0.125M Glycine. After two

153 washes with ice-cold PBS, cells were lysed using RIPA buffer (25 mM Tris-HCl, pH
154 7.5, 150 mM NaCl, 1% Triton X-100, 1% Na deoxycholate, 0.1% SDS, and 2 mM
155 EDTA, pH 8.0) containing protease inhibitors (Merck Millipore, #539134). Samples
156 were sonicated with the Misonix Sonicator 3000 Homogenizer (Mandel Scientific
157 Company Inc., Guelph, ON, Canada). To minimize non-specific binding, samples
158 were incubated with magnetic protein A/G (GE Healthcare Life Sciences) for 1 hour
159 at 4°C. Subsequently, the products were incubated overnight at 4°C with STAT3
160 (ABclonal, A19566) and IgG (Cell signaling, #2729) antibodies. The complexes were
161 precipitated by adding magnetic protein A/G for 1 hour at 4°C. After precipitation,
162 samples were washed with wash buffer. DNA products were extracted and eluted
163 using the QIAquick PCR purification kit (QIAGEN Inc., Valencia, CA, USA, Cat. No.
164 8106). The STAT3 binding fragments were identified using PCR, and the primer
165 details are listed in Supplementary Table 1.

166

167 **RNA pull-down assay**

168 The sense and anti-sense strands of biotin-labeled LOC344887 were generated using
169 the T7/SP6 transcription kit (Roche, Cat. No. 11685597910). The RNA lengths of
170 LOC344887-v1 and LOC344887-v2 generated by in vitro transcription were verified
171 using denaturing agarose gel electrophoresis with RNA Millennium™ markers (ABI,

172 #AM7150). The synthesized biotin-labeled RNA (3 μ g) was incubated with total
173 proteins (1000 μ g). After a 1-hour incubation at room temperature, the complex was
174 treated with ice-cold NT2 wash buffer and combined with 2x Laemmli loading buffer.
175 The samples were then subjected to SDS-PAGE. The signals of p-STAT3 (Tyr705)
176 and GAPDH were detected using X-ray films for chemiluminescence detection.

177

178 **RNA immunoprecipitation (RIP) assay**

179 The RIP assay was conducted following a previously described protocol [5]. Briefly,
180 cells were washed with ice-cold PBS and lysed with ice-cold polysomal lysis buffer
181 (100 mM KCl, 5 mM MgCl, 10 mM HEPES (pH 7.0), 0.5% NP-40, 1 mM DTT,
182 RNase inhibitor (Invitrogen, Cat. No. 10777019), and protease inhibitors (Merck
183 Millipore, #539134)). Samples were collected by centrifugation and pre-cleared with
184 magnetic protein-A/G beads (GE Healthcare Life Sciences). Immunoprecipitation (IP)
185 was carried out by adding STAT3 (ABclonal, A19566) and p-STAT3 Y705 antibody
186 (ABclonal, AP0705) at 4°C overnight. Each sample was incubated with magnetic
187 protein A/G beads for 1 hour at 4°C. Subsequently, complexes were washed with the
188 lysis buffer. To prevent DNA contamination, DNase I (Roche, Cat. No. 04716728001)
189 was incubated for 15 minutes at 37°C after washing. Total RNA was then extracted
190 using Trizol reagent.

191 ***In vitro* phosphatase assay**

192 The *in vitro* phosphatase assay followed a previously described protocol [6, 7]. In
193 brief, hepatoma cells were transfected with 3×FLAG-STAT3 plasmid for 72 h. After
194 transfection, total cell lysates were extracted and incubated with anti-FLAG M2
195 magnetic beads (Sigma) for 4 h. Then, the aliquoted sample was mixed with
196 recombinant human SHP-1 (R&D systems), LOC344887-v1, and v2 transcript. The
197 p-STAT3 (Tyr705) and total STAT3 expressions were determined via immunoblot
198 analysis.

199

200 **Duolink proximity ligation assay**

201 *In situ* proximity ligation assays (PLAs) were performed on fixed cells according to
202 the manufacturer's protocol (DUO92008, Sigma-Aldrich). Coverslips were initially
203 blocked for 45 minutes at 37°C with a blocking solution and then incubated with a
204 1:200 dilution of primary antibodies. SHP-1 antibody (Cell Signaling Technology,
205 #26516) alone was served as the negative control, while the interaction between
206 SHP-1 and p-STAT3 (Tyr705) was evaluated using both SHP-1 and p-STAT3 (Merck,
207 05485) antibodies at 4°C for overnight. Subsequently, the coverslips were washed
208 three times for 10 minutes each with PBS containing 0.1% Tween 20, followed by
209 incubation with secondary antibodies (PLA probes, Sigma-Aldrich) at 37 °C for 2

210 hours. After additional washing steps with buffer B, DNA ligase was added and
211 incubated at 37 °C for 30 minutes. A subsequent amplification step involved
212 incubation with DNA polymerase (DUO82030, Sigma-Aldrich) at 37 °C for 2 hours.
213 Finally, the coverslips were rinsed with buffer A and washed with 0.1× buffer B
214 before being mounted with a mounting solution containing DAPI. The close
215 proximity of these proteins, defined as less than 40 nm, is visualized by discrete red
216 fluorescent puncta under fluorescence microscopy.

217

218 **Supplementary figure legends**

219 **Supplementary Figure 1. Full-length sequences of the two LOC344887 variants**
220 **in HCC.** Upper panel: A schematic representation of LOC344887 variants in the
221 study, with the red line indicating the unique sequences for the v1 and v2 transcripts
222 of LOC344887. Lower panel: The full nucleotide sequences of LOC344887-v1 and
223 -v2 transcripts, identified by 5'RACE and 3'RACE, are shown. The distinctive
224 sequences between the two variants are marked in red.

225

226 **Supplementary Figure 2. Identification of LOC344887-mediated pathway.**

227 (A) A schematic workflow is illustrated for microarray profiling analysis using control
228 (sh-luc#1) and LOC344887-depleted (shLOC344887#1) J7 stable cell lines. (B)

229 Differentially expressed genes from LOC344887-silenced (shLOC344887#1) stable
230 cells as compared to control cells (sh-luc#1) were analyzed using KEGG pathway
231 analysis, revealing the top enriched pathways dysregulated under LOC344887
232 knockdown. (C) A table showing enrichment scores for differentially regulated
233 signaling pathways from LOC344887-depleted cells versus control cells.

234

235 **Supplementary Figure 3. Knockdown and overexpression of SHP-1 reciprocally**
236 **regulate cell motility of J7 cells.**

237 The impacts of SHP-1 (A) knockdown or (B) overexpression on cell motility of J7
238 cells were evaluated by transducing J7 cells with two SHP-1-specific shRNA, which
239 resulted in significantly increased numbers of migratory cells. Migratory cells stained
240 with crystal violet were subjected to quantification using ImageJ software, and
241 statistical significance was determined by one-way ANOVA followed by Tukey's
242 post-hoc test. The scale bar indicates 100 μm . **, $P < 0.01$.

243

244 **Supplementary Figure 4. Data analysis on LOC344887 knockdown microarray**
245 **data and GSE14520 identifies six potently dysregulated genes.**

246 (A) RNA was extracted from control (sh-luc#1) and LOC344887-depleted
247 (shLOC344887#1) cells and analyzed via microarray profiling. A Venn diagram

248 analysis revealed six differentially expressed genes in LOC344887-depleted J7 cells
249 and HCC dataset GSE14520 (intersection region), including high mobility group
250 AT-hook 2 (HMGA2), Tissue Factor Pathway Inhibitor (TFPI), CAMP-Regulated
251 Phosphoprotein 19 (ARPP19), SEC14 Like Lipid Binding 2 (SEC14L2), FXYD
252 Domain Containing Ion Transport Regulator 1 (FXYD1) and Kelch Repeat and BTB
253 Domain Containing 11 (KBTBD11). The selection criteria for target genes were: (1)
254 LOC344887#1/sh-luc#1 ratio > 2 , with $P < 0.05$ and $T/N < 0.83$, and (2)
255 LOC344887#1/sh-luc#1 ratio < 0.5 , with $P < 0.05$ and $T/N > 1.2$. (B) Relative
256 fold-change (shLOC344887#1/sh-luc#1) in the expression of the six potential target
257 genes regulated by LOC344887 are shown. (C) The expression intensity of the six
258 target genes in normal tissues (N) and HCC tissues (T) was examined. Statistical
259 significances were derived from the Mann-Whitney test. (D) Overall survival and
260 recurrence-free survival in relation to the expression of the six candidates were
261 analyzed using the publicly available GSE14520 dataset with Kaplan-Meier survival
262 analysis and log-rank tests, showing HMGA2 and TFPI as only two candidates
263 correlated with worse OS and RFS. Median expression values of these genes were
264 used as cutoffs. *, $P < 0.05$; **, $P < 0.01$. (E) The expression correlations between
265 LOC344887, HMGA2, and TFPI in HCC tissues were determined using Spearman's
266 rank correlation coefficient.

267 **Supplementary Figure 5. HMGA2 expression can be regulated by phosphatase**
268 **SHP-1 and STAT3 phosphorylation.**

269 Impacts of SHP-1 on HMGA2 expression were investigated by (A) knocking down or
270 (B) overexpressing SHP-1 and assessing for changes in HMGA2 protein levels. (C) A
271 dominant negative mutant of STAT3 (Y705F) was utilized to assess the role of STAT3
272 in mediating HMGA2 expression.

273

274 **Supplementary Figure 6. Clinicopathological correlations of LOC344887 to**
275 **p-STAT3 (Tyr705) and HMGA2 using HCC tissue array.**

276 (A) HCC tissue arrays that contain normal, cirrhosis, and HCC were utilized to
277 examine their correlation to p-STAT3 (Tyr705) and HMGA2 expression using
278 immunohistochemistry (IHC). The brown signals indicated the expression of
279 p-STAT3 (Tyr705) and HMGA2, showing significantly elevated expression of
280 p-STAT3 and HMGA2 in HCC when compared to normal or cirrhosis tissues—scale
281 bar: 100 μ m. Quantitative results and statistical significance were determined using
282 one-way ANOVA followed by Tukey's post-hoc test. *, $P < 0.05$; **, $P < 0.01$. (B) The
283 correlation between LOC344887 (RNA level), p-STAT3 (Tyr705) (protein level), and
284 HMGA2 (protein level) in HCC was evaluated using Spearman's rank correlation
285 coefficient, showing significant correlations among LOC344887, p-STAT3 (Tyr705)

286 and HMGA2.

287

288 **Supplementary Figure 7. HMGA2 promoter contains putative STAT3 binding**
289 **element responsible for LOC344887 in HCC.**

290 (A) Mutant construct (VII) and wild-type construct (VI) containing putative STAT3-2
291 binding site were transfected into Mahlavu control cells (sh-luc#1) or
292 LOC344887-depleted cells (shLOC344887#1) to demonstrate the importance of
293 STAT3-2 in LOC344887-mediated HMGA2 promoter activity. (B) The same reporter
294 constructs utilized in (A) were transfected into control (vc), LOC344887-v1 or
295 LOC344887-v2-overexpressing Huh7 cells, showing significantly enhanced HMGA2
296 promoter activities when either LOC344887 variant was overexpressed. Luciferase
297 reporter activities measured were normalized to vc and presented in fold changes, as
298 statistical significance was obtained from one-way ANOVA followed by Tukey's
299 post-hoc test. *, $P < 0.05$; **, $P < 0.01$.

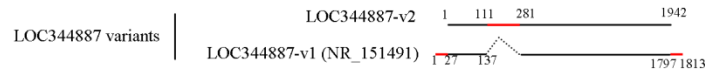
300

301 **References**

302 1. Hosono S, Lee CS, Chou MJ, Yang CS, Shih CH. Molecular analysis of the p53
303 alleles in primary hepatocellular carcinomas and cell lines. *Oncogene*. 1991; 6:
304 237-43.

- 305 2. Lin YH, Wu MH, Liu YC, Lyu PC, Yeh CT, Lin KH. LINC01348 suppresses
306 hepatocellular carcinoma metastasis through inhibition of SF3B3-mediated EZH2
307 pre-mRNA splicing. *Oncogene*. 2021; 40: 4675-85.
- 308 3. Liao CJ, Wu TI, Huang YH, Chang TC, Wang CS, Tsai MM, et al.
309 Glucose-regulated protein 58 modulates cell invasiveness and serves as a prognostic
310 marker for cervical cancer. *Cancer Sci*. 2011; 102: 2255-63.
- 311 4. Chan YL, Liao CL, Lin YL. Human Kinase/Phosphatase-Wide RNAi Screening
312 Identified Checkpoint Kinase 2 as a Cellular Factor Facilitating Japanese Encephalitis
313 Virus Infection. *Front Cell Infect Microbiol*. 2018; 8: 142.
- 314 5. Hsieh CL, Liu H, Huang Y, Kang L, Chen HW, Chen YT, et al. ADAR1
315 deaminase contributes to scheduled skeletal myogenesis progression via stage-specific
316 functions. *Cell Death Differ*. 2014; 21: 707-19.
- 317 6. Kim BR, Ha J, Kang E, Cho S. Regulation of signal transducer and activator of
318 transcription 3 activation by dual-specificity phosphatase 3. *BMB Rep*. 2020; 53:
319 335-40.
- 320 7. Liu C, Shen A, Song J, Cheng L, Zhang M, Wang Y, et al.
321 LncRNA-CCAT5-mediated crosstalk between Wnt/beta-Catenin and STAT3 signaling
322 suggests novel therapeutic approaches for metastatic gastric cancer with high Wnt
323 activity. *Cancer Commun (Lond)*. 2024; 44: 76-100.

324 **Supplementary Figures**

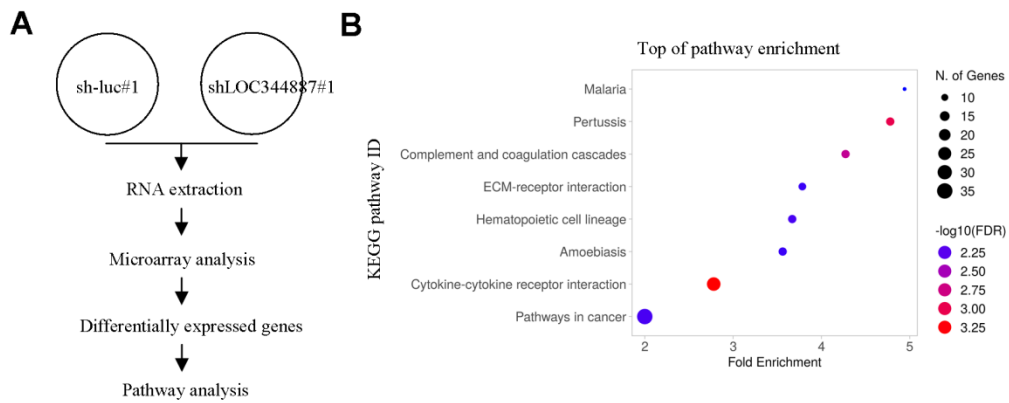


LOC344887-v1
ATAATTCTACCAGAGAAGAACACACGCATTTCGGCTGGTGTGCTGCTCCAGGG
 AAAGTTCTGTACTCCACTGACTCTCTTTCTGATAACATGGCCAGCAAGAAA
 GTAATTACAGTGTGGAGCAACAGGGGAAGTGGTGGCAGACTCCGCCAAGCA
 CTGGGTCTGAAGCAGTGGTGTACAGCGGCTGGAGAACGTCAAGCAGCTGAC
 GGATGGCAAGTGGAGTCCGCACCTTGACAGCAAGGGCAGGTGGAGAGTA
 CTTCTGGTCAATTGGCATCCCCATGACCAAGTCCCGTGGCGGCTACTTTGAA
 AACTTCTCGCGGCTGGCGCCGTGAAGCCTGTGATGGAGATTACTACACCT
 TGGTGTACCCGATGGAGATGTACCAATGGATGGTATCTCTGTTGCTGATTTGG
 AGCAGCCGCTCTAGCAITTTTAATTCTCCAGAGAAITTTAGGCAAGGCCGTG
 GGGCTCAGTGCAGAAGCACTAACAAATACAGCAATATGCTGATGTTTGTCCAAGG
 TTTTGGGAAAGAAATCCGAGATGCAAGAITACCCCGGAAGCTTTCGAGAAGC
 TGGGATCCCTGCAGCAAGGAAATAGCCAATATGTGTCGTTTCTATGAAATGAA
 GCCAGCCGAGATGTCAATCTCACCCACCACTAAATCCCAAAGTCAAAGCTTC
 AGCCAGTTTATCTCAGAGAACAGGGAGCCTTCAAGGGCATGTAGAAAATCAGC
 TGTTCAGATAGGCCCTGCACCACACAGCCTTTTCTCTGATCCTTTTCTCTT
 TACGGCACAACTTATGTTGACAGAACATGCTGGAATGCAAITGTTGCAACAC
 CGAAGGATTTCTGCGGTCGCTCTCAGTAGGAAGCACTGCATTGGTATAGAA
 CACGGTAATTTGATTACATTTAACTTGTAGTTAGTATAAGGGTGGTACACCT
 GTTTGGTAAAATGAGAAAGCCTCGGAACTTGGAGCTTCTCTACCCTAATGGG
 AGGGCAGATTACTGGGATTTCTCTGGGTGAGTAATTTCAAGCCCTAATGCTG
 AAATCCCCTAGGCAGCTCCAGTTTCTCACTGCATTGCAAAATCCAGTGA
 CTTTTAAGTACTTTTAACTTAAAAAATGAACATCTTTGTAGAGAATTTCTGGGG
 AACATGGTGTCAATGAACAAGCACAAGCAATGGAAATGCTAAAATCAGTTTTG
 CCTCAAGATTGGAAGTTATTTTCTGACTATTCATGAAGTCTATTGAGCCAC
 CATTCAATTATTCATCTAATAATCCTTGATCCTTCAATTTATCCATTGCAAACT
 TTCTGAGCACCAGCAGGGTGGCCATTTGGGACTTCTCTCATTCTATGTGTT
 TTCTTAAAGTATCCACTCTCGAAAGGCTCCTTCCAGTCTGTGGTGGGTTCA
 AAGTCATGCCAGGGCCAGGGGGCCATCTCTCGTTTAGCTCTAGGCCAAAATCCA
 GGGGATCTCAGTGGGAGCGGGGCGAGGAGCTGGAGGGAAGGCTGTGAAG
 GGTAGGGATGTGGAAGACAAGGTGACAGAGGACCCAATAGGACCTTTCTATA
 TCTCTGGCTAGCAATTTCTACATCATATTGTAATCGTCTAATTTGCTAGTTTCTT
 CCTTACTGTGAGTGACTAACAGTCACTTTATCCAGTGCCTGGTACATAATAAGT
 GATCAATAAATGTTGATTGACTAAATGAGTAAAAA
AAAAAAAAAAAAAAAAAAAA

LOC344887-v2
 GCATTTCGGCTGGTGTGCTGCTCCAGGGAAAGTTCGTACTCCACTGACTCTCT
 CTTTTCTGATAACATGGCCAGCAAGAAAGTAATTACAGTGTGGGAAACAGG
AGCTCAAGGTGGCTCTGTGGCAGGGCAATTTTGGAGGCAAAAAATTTGCAGT
GAGAGCAGTGACCAGGGATGTGACTTGACCAAAATGCCTGGAGCTCCAGCGCT
TGGAGCTGAGGTGGTCAAAGGTGACCTGAATGATAAAGCATCGGTGGACAGTGC
CTTAAAAGGGAAAGTGGTGGCAGACTCCGCCAAGCACCTGGGTCTGAAGCACG
 TGGTGTACAGCGGCTGGAGAACGTCAAGCAGCTGACGGATGGCAAGCTGGAGG
 TGCCGCACTTGACAGCAAGGGCAGGTGGAGGAGTACTTCTGGTCAATTGGCAT
 CCCCATGACCAGTGTCCCGTGGCGGCTACTTTGAAAATTTCTCGCGGCTGG
 CGGCCGTGAAGCCTGTATGGAGATTACTACACCTTGGGTGACCCGATGGGAG
 ATGTACCAATGGATGGTATCTCTGTTGCTGATTTGGAGCAGCGCTCTAGCAT
 TTTAATTCTCAGAGGAAITTTAGGCCAAGGCCGTGGGGCTCAGTGCAGAAAGCAC
 TAACAATACAGCAATATGCTGATGTTTGTCCAAGGTTTGGGAAAGAAAGTCCG
 AGATGCAAAGATTACCCCGAAGCTTTCGAGAAGTGGGATTCCTGCAGCAAA
 GGAATAGCCAATATGTGCTGTTTCTATGAAATGAAGCCAGACCGAGATGCAAT
 CTCACCACCACTAAATCCCAAAGTCAAAGCTTCAAGCAGTTTATCTCAGAGA
 ACCAGGGAGCCTTCAAGGGCATGTAGAAAATCAGTGTTCAGATAGGCCCTCTGC
 ACCACACAGCCTTTCTCTGATCCTTTCTCTTACGGCACAACTTATGAT
 TTGACAGAACATGCTGGAATGCAATTTGTTGCAACCCGAAGGATTTCTGCGGT
 CGCTCTTCAAGTAGGAAGCACTGCATTGGTATAGAACACCGGTAATTTGATTCAC
 ATTTAACTGTAGTTAGTATAAGGGTGGTACACCTGTTTGGTAAAATGAGAAG
 CTTGGAACTGGAGCTTCTCTACCCTAATGGGAGGGCAGATTATCTGGG
 ATTTCTCTGGGTGAGTAAITTCAGGCCCTAATGCTGAAATTTCCCTAGGCAGCTC
 CAGTTTTCTCAACTGCATTGCAAAATCCAGTGAACITTTAAGTACTTTTAACTT
 AAAAAATGAACATCTTTGTAGAGAATTTCTGGGGAACATGGTGTCAATGAAC
 AAGCACAAGCATTGGAAATGCTAAAATCAGTTTGGCTCAAGATTGGAAAGTTTA
 TTTCTGACTCATTGAAAGTCACTATTGAGCCACCATTCATTAATTCATCTAT
 TAATTCCTTGATCCTTATTATCCATTCTGCAAACTTTCTGGAGCACCAGCAG
 GGTGGCCATTTGGGACTTCTTCTCATTCTATGTGTTTCTTAAAGTGTATCC
 ACTCTGAAAGGCTCTTCCAGTCTGTGGTGGGTTCAAGTATGCAAGGGCCCA
 GGGGGCCATCTCTCGTTTAGCTTAGGCCAAAATCCAGGGGATCTGCAAGTGGGG
 AGCGGGGCAAGAAAGTGGAGGGAAGGCTGTGAAGGTAGGGATGTGGAAAG
 ACAAGGTGACAGAAGGACCAATAGGACCTTCTATATCTGGCTTAGCAITTT
 CTACATCATATTGTAATCGTCTATTGCTAGTTTCTCTTACTGTGAGTGACTA
 ACAGTCACTTTATCCAGTGCCTGGTACATAAATGATGATCAATAAATGTTGAT
 TGACTAAATGAGTAAA

Supplementary Figure 1

325
 326
 327
 328



C The differential signaling in LOC344887-depleted J7 and control cell

Signaling	Fold enrichment	Enrichment FDR
KEGG_Malaria	4.94136	0.00671
KEGG_Pertussis	4.77882	0.001
KEGG_Complement and coagulation cascades	4.27282	0.00215
KEGG_ECM-receptor interaction	3.78323	0.00622
KEGG_Hematopoietic cell lineage	3.66859	0.00596
KEGG_Amoebiasis	3.56069	0.00622
KEGG_Cytokine-cytokine receptor interaction	2.77951	0.00054
KEGG_Pathways in cancer	1.99868	0.00596

Abbreviations: KEGG, Kyoto encyclopedia of genes and genomes.

Supplementary Figure 2

329

330

331

332

333

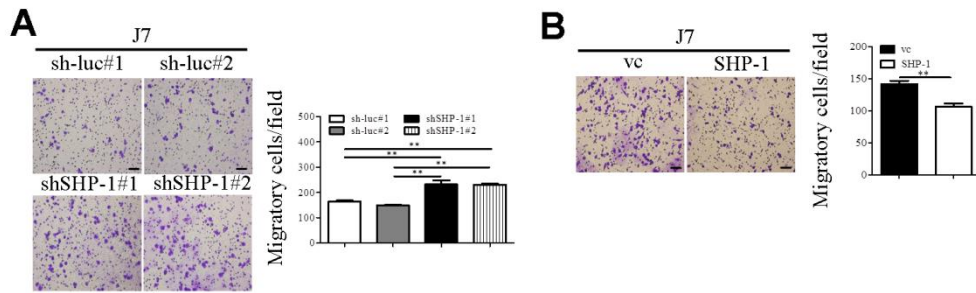
334

335

336

337

338



Supplementary Figure 3

339

340

341

342

343

344

345

346

347

348

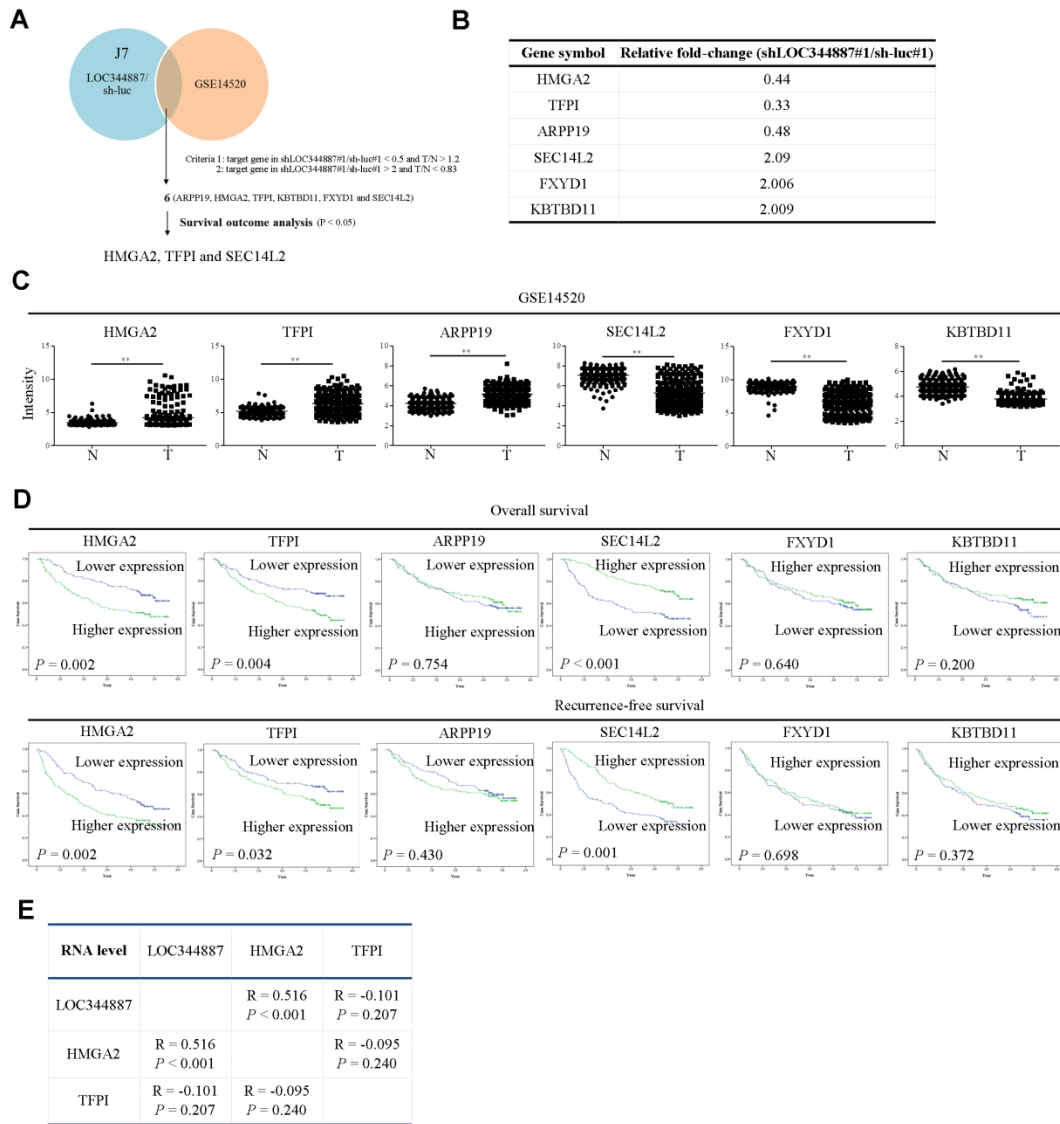
349

350

351

352

353



Supplementary Figure 4

354

355

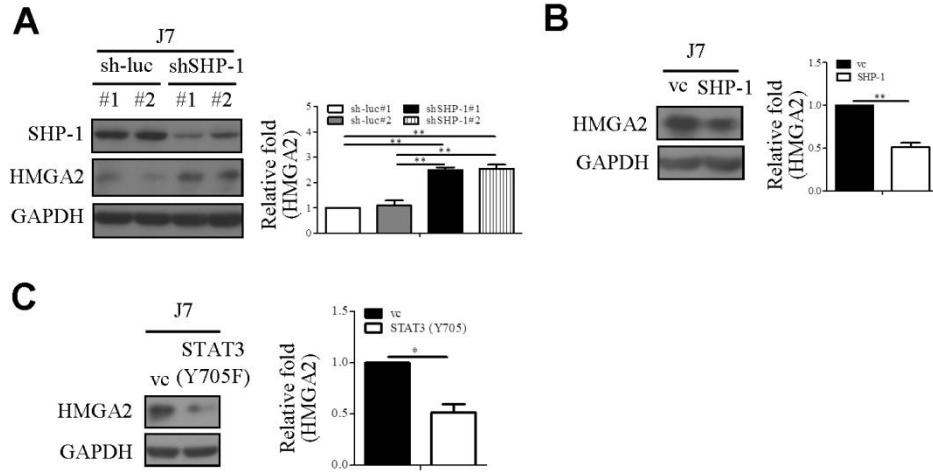
356

357

358

359

360



Supplementary Figure 5

361

362

363

364

365

366

367

368

369

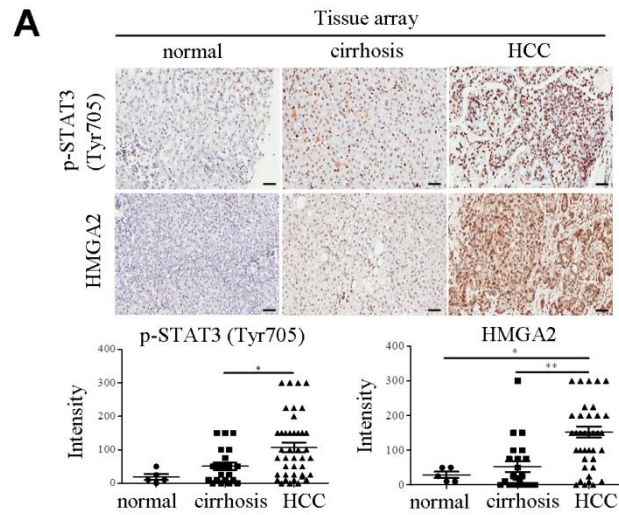
370

371

372

373

374



B

	LOC344887 (RNA level)	p-STAT3 Tyr705 (protein level)	HMGA2 (protein level)
LOC344887 (RNA level)		r = 0.310 P = 0.048	r = 0.325 P = 0.038
p-STAT3 Tyr705 (protein level)	r = 0.310 P = 0.048		r = 0.507 P < 0.001
HMGA2 (protein level)	r = 0.325 P = 0.038	r = 0.507 P < 0.001	

Supplementary Figure 6

375

376

377

378

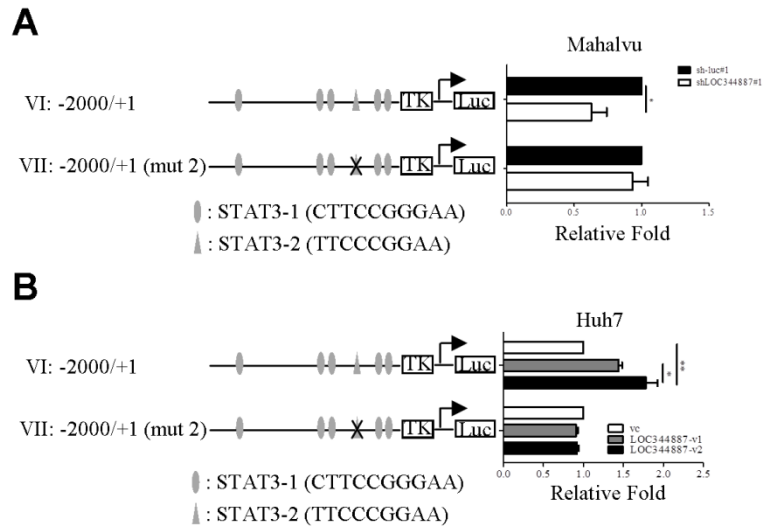
379

380

381

382

383



Supplementary Figure 7

384
385
386
387
388
389
390
391
392
393
394
395
396
397
398
399
400
401
402
403
404
405
406
407

408 Supplementary Table 1. The primers were used in RT-PCR, qRT-PCR, ChIP and
409 shRNA analysis.

RT-PCR

LOC344887 forward primer: 5'- CTCTCTCTTTTCCTGATAAC-3'

LOC344887 reverse primer: 5'- AATATCAGCAACAGAGATAC-3'

18S rRNA forward primer: 5'- CGAGCCGCCTGGATACC-3'

18S rRNA reverse primer: 5'- CCTCAGTTCGAAAACCAACAA-3'

qRT-PCR

LOC344887 forward primer: 5'-GAGCCTTCAAGGGCATGTAGA-3'

LOC344887 reverse primer: 5'-GAATGTTGTGCCGTAAAGAGGAA-3'

Specific LOC344887-v1 forward primer: 5'-ATAATTCTCACCAGAGAAGAAACA-3'

Specific LOC344887-v1 reverse primer: 5'-TCAGTGGAGTAACAGAACTTTCC-3'

Specific LOC344887-v2 forward primer: 5'-CTGTGGCCAGGGCAATTTT-3'

Specific LOC344887-v2 reverse primer: 5'-CTCCAGGGCATTGTTGTC-3'

HMGA2 forward primer: 5'- TGGGAGGAGCGAAATCTAA -3'

HMGA2 reverse primer: 5'- GGTGAACTCAAGCCGAAG -3'

TFPI forward primer: 5'- GTGGATGCCTGGGCAATA -3'

TFPI reverse primer: 5'- GGAAACCATTCGGACCATCT -3'

18S rRNA forward primer: 5'- CGAGCCGCCTGGATACC-3'

18S rRNA reverse primer: 5'- CCTCAGTTCGAAAACCAACAA-3'

ChIP assay

HMGA2 promoter forward-2 primer: 5'-TGTCAGGGGACCTCTCCCAC-3'

HMGA2 promoter reverse-2 primer: 5'-GAGGTCACCCCTGGGCAGTT-3'

GAPDH forward primer: 5'-TACTAGCGGTTTTACGGGCG-3'

GAPDH reverse primer: 5'-TCGAACAGGAGCAGAGAGCGA-3'

shRNA

LOC344887 shRNA-1 forward:

5'-CCGGATACAGCAATATGCTGATGTTCTCGAGAACATCAGCATATTGCTGTAT
TTTTT-3'

LOC344887 shRNA-1 reverse:

5'-AATTA AAAAATACAGCAATATGCTGATGTTCTCGAGAACATCAGCATATTG
CTGTGT-3'

LOC344887 shRNA-2 forward:

5'-CCGGCTCAACCAAGATAAGGAAGTGCTCGAGCACTTCCTTATCTTGGTTG
AGTTTTT-3'

LOC344887 shRNA-2 reverse:

5'-AATTAAAACTCAACCAAGATAAGGAAGTGCTCGAGCACTTCCTTATCTT
GGTTGAG-3'

410

411

412

413

414

415

416

417

418

419

420

421

422

423

424

425

426

427

428 Supplementary Table 2. The antibodies were used in western blot analysis, IHC, PLA
 429 and RIP assay.

Antibody	Company	Catalog No.	Dilution/Concentration	Assay
HMGA2	Cell Signaling	#5269	1:1000	WB
			1:100	IHC
p-STAT3 (Tyr705)	Cell Signaling	#9145	1:1000	WB
STAT3	Cell Signaling	#9139	1:1000	WB
SHP-1	Cell Signaling	#26516	1:200	PLA
p-STAT3 (Tyr705)	Merck	05485	1:200	PLA
p-STAT3 (Tyr705)	ABclonal	AP0705	3 µg	RIP
			1:100	IHC
STAT3	ABclonal	A19566	3 µg	RIP
SHP-1	ABclonal	A19111	1:1000	WB,
GAPDH	Santa Cruz	sc-47724	1:8000	WB

430